The Astrophysical Journal Letters, 739:L18 (6pp), 2011 September 20 doi:10.1088/2041-8205/739/1/L18
© 2011. The American Astronomical Society. All rights reserved. Printed in the U.S.A.

A DEEP RADIO SURVEY OF HARD STATE AND QUIESCENT BLACK HOLE X-RAY BINARIES

J. C. A. Miller-Jones[1,6], P. G. Jonker[2,7,8], T. J. Maccarone[3], G. Nelemans[4], and D. E. Calvelo[5]
[1] International Centre for Radio Astronomy Research, Curtin University, GPO Box U1987, Perth, WA 6845, Australia; james.miller-jones@curtin.edu.au
[2] SRON, Netherlands Institute for Space Research, 3584 CA, Utrecht, The Netherlands
[3] School of Physics and Astronomy, University of Southampton, Highfield SO17 IBJ, UK
[4] Department of Astrophysics, IMAPP, Radboud University Nijmegen, Heyendaalseweg 135, 6525 AJ, Nijmegen, The Netherlands
[5] School of Physics and Astronomy, University of Southampton, Highfield SO17 IBJ, UK
Received 2011 April 15; accepted 2011 May 31; published 2011 August 29

ABSTRACT

We have conducted a deep radio survey of a sample of black hole X-ray binaries in the hard and quiescent states to determine whether any systems were sufficiently bright for astrometric follow-up with high-sensitivity very long baseline interferometric arrays. The one hard-state system, Swift J1753.5−0127, was detected at a level of 0.5 mJy beam^{-1}. All 11 quiescent systems were not detected. In the three cases with the highest predicted quiescent radio brightnesses (GRO J0422+32, XTE J1118+480, and GRO J1655−40), the new capabilities of the Expanded Very Large Array were used to reach noise levels as low as 2.6 μJy beam^{-1}. None of the three sources were detected to 3σ upper limits of 8.3, 7.8, and 14.2 μJy beam^{-1}, respectively. These observations represent the most stringent constraints to date on quiescent radio emission from black hole X-ray binaries. The uncertainties in the source distances, quiescent X-ray luminosities at the times of the observations, and the power-law index of the empirical correlation between radio and X-ray luminosities make it impossible to determine whether these three sources are significantly less luminous in the radio band than expected. Thus it is not clear whether that correlation holds all the way down to quiescence for all black hole X-ray binaries.

Key words: black hole physics – ISM: jets and outflows – radio continuum: stars – X-rays: binaries

1. INTRODUCTION

Black hole X-ray binaries spend the majority of their duty cycles in a low-luminosity ($<10^{33.5}$ erg s^{-1}), quiescent state. Theoretical models to explain the low luminosities and the observed spectra either consider radiatively inefficient accretion flows (e.g., Narayan & Yi 1995), reduce the inner accretion rate to zero (Narayan et al. 2000; Quataert & Gruzinov 2000), invoke winds or outflows (Blandford & Begelman 1999), or some combination of these effects. More recently, jets have been demonstrated to represent a significant component of the power output of accreting black holes at low luminosities (Fender et al. 2003; Gallo et al. 2005a), making the coupling between inflow and outflow processes crucial to understanding the nature of low-luminosity accretion.

Simultaneous multi-wavelength observations (Gallo et al. 2003; Corbel et al. 2003) have shown that the radio and X-ray luminosities (L_R and L_X, respectively) of hard state black hole X-ray binaries are correlated via the nonlinear relation $L_R \propto L_X^{0.6}$, implying a fundamental coupling between the accretion and ejection processes in hard state systems, which was later demonstrated to extend unbroken into the quiescent state (Gallo et al. 2006). With the inclusion of a mass term, the correlation was further extended to include supermassive black holes (Merloni et al. 2003; Falcke et al. 2004; Gültekin et al. 2009). However, the universality of this correlation has been called into question. From an observational perspective, a population of radio-faint X-ray binaries lying well below the correlation was discovered in the relatively bright hard X-ray state (e.g., Gallo 2007), although Coriat et al. (2011) found evidence that this population may rejoin the correlation at low luminosities ($\lesssim 5 \times 10^{-5} L_{\rm Edd}$). More theoretical work also suggested that the correlation should break down below a fraction 10^{-5} of the Eddington luminosity $L_{\rm Edd}$, with the power-law index steepening as the synchrotron X-ray emission from the jet begins to dominate the Compton-upscattered emission from the accretion flow (Yuan & Cui 2005). Although two of the most sub-Eddington systems detected in the radio band, Sgr A* and A0620-00, both appear to rule out this model, it is possible that the proposed threshold luminosity below which the correlation steepens is either significantly lower than proposed by Yuan & Cui (2005), or that it is not the same for all sources. Thus, the true nature of the coupling between inflow and outflow at the lowest luminosities has been difficult to confirm.

The extremely low luminosity of the quiescent state of black hole X-ray binaries has rendered it inaccessible to radio observations for all but the closest and brightest systems, A0620-00 and V404 Cyg, respectively. A0620-00, at a distance of only $d = 1.06 \pm 0.12$ kpc (Cantrell et al. 2010), is currently the faintest radio-emitting black hole X-ray binary known, with a measured 8.5 GHz radio flux density of 51 ± 7 μJy and a simultaneously determined 2–10 keV X-ray luminosity of only $7.1 \times 10^{30} (d/1.2\,{\rm kpc})^2$ erg s^{-1} (Gallo et al. 2006). V404 Cyg, at the recently measured parallax distance of 2.39 ± 0.14 kpc (Miller-Jones et al. 2009), has a relatively high quiescent luminosity of 4×10^{32} erg s^{-1} (Corbel et al. 2008). It is a persistent radio source with a flat radio spectrum (Gallo et al. 2005b) and a flux density of ∼0.3 mJy, although occasional small flares have been detected in the quiescent state, in which the flux density increases by a factor of three on timescales of ∼30 minutes (Miller-Jones et al. 2008). The persistent radio emission is believed to arise from a steady, partially self-absorbed, compact jet (e.g., Blandford & Konigl 1979). The persistent, core-dominated nature of this

[6] Also at NRAO Headquarters, 520 Edgemont Road, Charlottesville, VA 22903, USA.
[7] Also at Harvard-Smithsonian Center for Astrophysics, 60 Garden Street, Cambridge, MA 02138, USA.
[8] Also at Department of Astrophysics, IMAPP, Radboud University Nijmegen, Heyendaalseweg 135, 6525 AJ, Nijmegen, The Netherlands.

emission makes black hole X-ray binaries ideal astrometric targets when they are in their hard or quiescent states. High-precision astrometric observations with very long baseline interferometry (VLBI) would allow us to measure source proper motions, which can provide information about the formation mechanisms of the black holes (e.g., Mirabel et al. 2001; Mirabel & Rodrigues 2003), and in some cases, model-independent distances (e.g., Miller-Jones et al. 2009). Prior to embarking on an astrometric campaign, we need to determine which hard state and quiescent systems are bright enough to be detected with the High Sensitivity Array (HSA).

While several black hole X-ray binaries have been monitored during their decay to quiescence following an outburst (e.g., Jonker et al. 2004, 2010), in every case, the sources have faded below the detection threshold before reaching their stable quiescent luminosity. Using the enhanced sensitivity of the new wideband receiver (CABB; the Compact Array Broadband Backend) on the Australia Telescope Compact Array (ATCA), Calvelo et al. (2010) attempted to detect the two quiescent systems GRO J1655−40 and XTE J1550−564, finding mildly constraining 3σ upper limits on their quiescent radio emission of 26–27 μJy at 5.5 GHz and 47 μJy at 9 GHz. Deeper radio observations are required to identify astrometric targets and to accurately determine the nature of the correlation between radio and X-ray emission in the quiescent state.

In this Letter, we describe a deep radio survey of quiescent black hole X-ray binaries carried out by the Very Large Array (VLA) in order to identify possible targets for an astrometric observing campaign, assuming the existence of more radio-loud quiescent sources similar to A0620-00, V404 Cyg, and Sgr A*. We also report on higher-sensitivity follow-up observations of three targets using the wide bandwidths now available with the Expanded Very Large Array (EVLA; Perley et al. 2011).

2. OBSERVATIONS AND DATA REDUCTION

2.1. VLA

In order to identify possible targets for an astrometric VLBI campaign, we observed 11 quiescent black hole X-ray binaries using the old VLA system under program code AM986. The integration times were set to provide a robust detection of the minimum flux density for which an astrometric detection with the HSA would be possible, equating to $\sim$5 hr of time on source with the VLA. The schedules were submitted to the dynamic queue as a series of 1 hr blocks, such that between one and five epochs of observation were taken for each source. The observation log is shown in Table 1. The observations were made at a frequency of 8.46 GHz, in dual circular polarization mode, with 100 MHz of bandwidth split equally between two intermediate frequency (IF) pairs. The array was in its CnB and C configurations.

Data were reduced using the 31Dec08 version of the Astronomical Image Processing System (AIPS) software package (Greisen 2003). Since the data were taken during the transition to the EVLA, the array comprised between 20 and 22 upgraded EVLA antennas. Baseline-based calibration was used to account for the mismatch between the bandpasses of the old VLA antennas and the new EVLA antennas. The flux density scale was set using one of the primary flux calibrators J1331+3030 or J0137+3309, using the coefficients derived by NRAO staff at the VLA in 1999.2. Phase calibration was performed using the calibrator sources listed in Table 1. The calibration was applied to the target data, which were imaged, deconvolved, and subjected to self-calibration in cases where the field contained sufficient flux to adequately constrain the solutions.

2.2. EVLA

Following the non-detection of all 10 quiescent black hole systems during the VLA campaign, we used the nominal source distances and measured quiescent X-ray luminosities of the sources to identify the three targets with the highest quiescent flux densities predicted from the radio/X-ray correlation of Gallo et al. (2006); XTE J1118+480, GRO J0422+322 and GRO J1655−40. These sources were observed under program AM1014 with the EVLA (Perley et al. 2011), via the Resident Shared Risk Observing (RSRO) scheme. We observed in the 4–8 GHz receiver band with an observing bandwidth of 2.048 GHz. The observations used two 1024 MHz basebands centered at 5.38 and 6.80 GHz, thus providing the most contiguous possible frequency coverage while avoiding radio frequency interference known to exist below 4.5 GHz and between 5.93 and 6.27 GHz. Each baseband was split into eight 128 MHz sub-bands. Data were taken in dual circular polarization mode, using 5 s integrations. The array was in its C-configuration, sufficiently extended to ensure that confusion did not prevent us reaching the expected thermal noise-limited sensitivity levels.

Data reduction was performed using the Common Astronomy Software Applications (CASA) package (McMullin et al. 2007). Bandpass and flux density calibration were performed using the primary flux calibrator (J0137+3309 for GRO J0422+32, and J1331+3030 for XTE J1118+480 and GRO J1655−40). The amplitude scale was set according to the Perley–Butler coefficients derived from recent measurements at the EVLA. Amplitude and phase gains were derived for all calibrator sources, and the phase calibrators used are shown in Table 1. Finally, the calibration was applied to the target sources, which, following frequency averaging by a factor of eight, were then subjected to several rounds of imaging and phase-only self-calibration. To successfully image and deconvolve such wide bandwidths, we used the CASA implementation of the Sault–Wieringa algorithm for multi-frequency synthesis imaging (Sault & Wieringa 1994).

3. RESULTS

In our original VLA survey, only Swift J1753.5−0127 was detected, with a flux density of 0.4–0.5 mJy in each of the observations (the exact flux densities have already been reported by Soleri et al. 2010). The other 10 sources were not detected, and are therefore too faint for an astrometric HSA observing campaign. Of the three systems that we observed with the EVLA (GRO J0422+32, XTE J1118+480, and GRO J1655−40), none were detected at a statistically significant level. The observations of GRO J1655−40 were hampered by the array configuration (C configuration; given the low declination of the source, a hybrid array with an extended northern arm would have been more appropriate) and the presence of significant extended emission in the field. To filter this out, we selected only data with a *uv*-spacing of >5 kλ. Our best radio upper limits on all 11 sources in our sample are shown in Table 2.

While not formally significant, the measured radio brightnesses at the known source positions of XTE J1118+480 and GRO J1655−40 were 6.4 ± 2.6 and 9.0 ± 4.7 μJy beam^{-1}, respectively. This suggests that these are good candidates for deeper observations, using either longer integration times or further increased bandwidth following the completion

Table 1
Observation Log for the VLA and EVLA Observations of our Sample of Quiescent Black Hole X-ray Binaries

Source	Calibrator	Date	MJD	Bandwidth (MHz)	Time on Source (minutes)	Image Noise (μJy beam^{-1})
GRO J0422+322	J0414+3418	2009 Jun 21	55003.66 ± 0.15	100	99.0	28.7
		2009 Jun 22	55004.82 ± 0.02	100	50.2	...[a]
		2009 Jun 25	55007.52 ± 0.02	100	50.3	31.7
		2009 Jun 26	55008.76 ± 0.02	100	50.0	14.6
		2010 Nov 15	55515.14 ± 0.07	2048	148.6	2.8
XTE J1118+480	J1126+4516	2009 Jun 2	54984.10 ± 0.10	100	237.7	9.6
		2010 Nov 24	55524.53 ± 0.06	2048	142.5	2.6
GRO J1655−40	J1607−3331	2010 Dec 13	55543.77 ± 0.06	2048	146.7	4.7
H1705−250	J1751−2524	2009 Jun 15	54997.30 ± 0.08	100	122.2	16.4
		2009 Jun 16	54998.19 ± 0.02	100	44.0	31.0
		2009 Jun 19	55001.26 ± 0.02	100	48.8	27,6
		2009 Jun 30	55012.19 ± 0.02	100	43.2	27.7
Swift J1753.5−0127	J1743−0350	2009 Jun 9	54991.41 ± 0.02	100	47.5	21.7
		2009 Jun 10	54992.41 ± 0.02	100	47.2	46.6
		2009 Jun 15	54997.40 ± 0.02	100	46.2	23.0
XTE J1817−330	J1820−2528	2009 Jul 12	55024.24 ± 0.02	100	48.5	32.3
		2009 Aug 3	55046.20 ± 0.04	100	94.8	20.3
		2009 Aug 8	55051.19 ± 0.02	100	46.3	27.6
		2009 Aug 15	55058.15 ± 0.02	100	48.5	28.1
XTE J1818−245	J1820−2528	2009 Jul 7	55019.19 ± 0.02	100	50.2	25.6
		2009 Jul 15	55027.27 ± 0.02	100	50.0	29.8
		2009 Jul 23	55035.23 ± 0.02	100	50.0	26.5
		2009 Jul 24	55036.14 ± 0.02	100	65.0	21.7
		2009 Aug 8	55051.15 ± 0.02	100	47.7	25.4
V4641 Sgr	J1820−2528	2009 Jul 1	55013.15 ± 0.02	100	50.2	29.7
		2009 Jul 23	55035.27 ± 0.02	100	48.2	28.1
		2009 Aug 8	55051.11 ± 0.02	100	50.0	25.7
XTE J1859+226	J1850+2825	2009 Jun 5	54987.57 ± 0.02	100	47.5	23.8
		2009 Jun 6	54988.57 ± 0.02	100	47.2	23.6
		2009 Jun 7	54989.56 ± 0.02	100	47.2	23.3
		2009 Jun 8	54990.56 ± 0.02	100	47.2	22.8
		2009 Jun 10	54992.50 ± 0.02	100	43.2	52.6
XTE J1908+094	J1922+1530	2009 Jun 10	54992.45 ± 0.02	100	44.0	49.6
		2009 Jun 11	54993.45 ± 0.02	100	47.3	25.7
		2009 Jun 15	54997.48 ± 0.06	100	131.5	17.4
		2009 Jun 18	55000.45 ± 0.02	100	47.0	39.9
GS 2000+25	J1931+2243	2009 Jun 12	54994.53 ± 0.04	100	86.7	15.8
		2009 Jun 13	54995.57 ± 0.02	100	44.2	22.1
		2009 Jun 14	54996.50 ± 0.04	100	86.7	15.9
XTE J2012+381	J2015+3710	2009 Jun 6	54988.61 ± 0.02	100	44.3	21.3
		2009 Jun 7	54989.61 ± 0.02	100	44.3	23.5
		2009 Jun 9	54991.54 ± 0.04	100	89.0	16.2
		2009 Jun 10	54992.54 ± 0.02	100	44.3	40.2

Notes. Observations with 100 MHz of bandwidth were taken with the old VLA system, whereas those with 2048 MHz of bandwidth were taken with the new wideband capabilities of the EVLA.
[a] Phase connection was too poor to allow for calibration.

of the EVLA upgrade. Considering the entire sample, a Kolmogorov–Smirnov test on all 11 non-detections gave a probability of 0.126 that the measured pixel values at the source positions (as a fraction of the image noise) are consistent with the expected Gaussian distribution of zero mean and unit standard deviation. Thus, we cannot formally exclude the slightly positive pixel values at the positions of XTE J1118+480 and GRO J1655−40 being due to chance.

For all the systems in our sample with constraints on the quiescent X-ray luminosity, we have plotted our radio upper limits on the radio/X-ray correlation in Figure 1, together with a sample of other sources from the literature. We used WebPimms[9] to convert all X-ray luminosities to a 3–9 keV range, for compatibility with the observations of V404 Cyg and GX 339−4 that form the bulk of the sample (Corbel et al. 2003, 2008). We calculated the 8.4 GHz radio luminosities by multiplying the measured monochromatic luminosities by a nominal observing frequency of 8.4 GHz, assuming a flat radio spectrum in all cases. We performed a fit to the correlation using data from A0620-00, GX 339−4, and V404 Cyg, finding $L_{\rm R} \propto L_{\rm X}^{0.67}$. All three of our EVLA upper limits fall on or above our best fitting correlation, so we cannot constrain whether the correlation continues to hold at the lowest luminosities.

4. DISCUSSION

The only quiescent sources with radio detections are A0620-00 (Gallo et al. 2006) and V404 Cyg (Gallo et al.

[9] http://heasarc.gsfc.nasa.gov/Tools/w3pimms.html

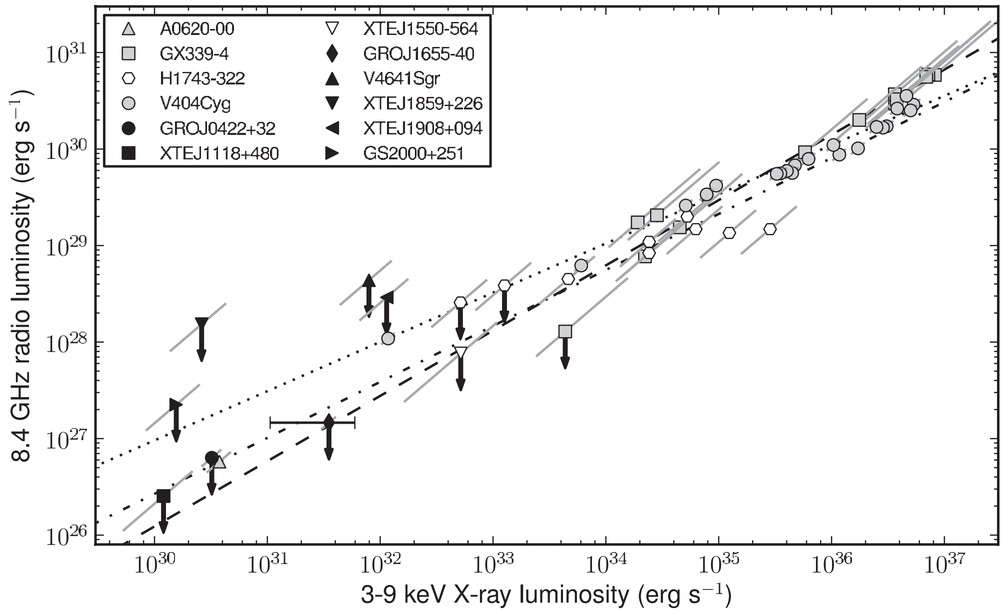

Figure 1. Measured radio and X-ray luminosities of black hole X-ray binaries in the hard and quiescent states. Black markers show the sources studied in this work. Gray diagonal error bars show the effect of distance uncertainties on the source position in this plane. The horizontal error bar for GRO J1655−40 shows the measured range of X-ray luminosity for this source. The dashed line shows the best-fitting correlation ($L_{\rm R} \propto L_{\rm X}^{0.67}$) for the three sources A0620-00, V404 Cyg, and GX 339−4 (indicated by gray markers) taken together. Open markers show other points from the literature for which both simultaneous radio and X-ray observations and distance constraints are available (Corbel et al. 2003,2008; Gallo et al. 2006; Calvelo et al. 2010; Coriat et al. 2011). Dotted line shows the correlation found by Corbel et al. (2008) for V404 Cyg. Dot-dashed line shows the correlation fitted by Gallo et al. (2006). The hard-state radio-quiet outliers from the correlation (e.g., Swift J1753.5−0127; Gallo 2007; Soleri et al. 2010) have been omitted for clarity.

Table 2
Quiescent Luminosities and Final 3σ Upper Limits on Radio Emission from our Sample of Black Hole X-ray Binaries, After Stacking All Data on Each Source

Source	Distance (kpc)	Stellar Type	$L_{3-9\,{\rm keV}}$ (erg s^{-1})	3σ Radio Upper Limit (μJy beam^{-1})	$L_{8.4\,{\rm GHz}}$ (erg s^{-1})	Reference
GRO J0422+322	2.75 ± 0.25	M2V	3.2×10^{30}	8.3	$<6.3 \times 10^{26}$	G01
XTE J1118+480	1.8 ± 0.6	K5/M0V	1.2×10^{30}	7.8	$<2.5 \times 10^{26}$	M03
GRO J1655-40	3.2 ± 0.2	F3/F5IV	1.0–6.0 $\times 10^{31}$	14.2	$<1.5 \times 10^{27}$	G01, K02, H03, P08, C10
H1705-250	8.6 ± 2.0	K3/7V	$<10^{33}$	36.1	$<2.7 \times 10^{28}$	M99
XTE J1817−330				38.5		
XTE J1818−245				33.5		
V4641 Sgr	9.6 ± 2.4	B9III	8.0×10^{31}	47.3	$<4.4 \times 10^{28}$	T03
XTE J1859+226	6.3 ± 1.7		2.6×10^{30}	38.4	$<1.5 \times 10^{28}$	T03
XTE J1908+094	∼8.5		$\sim1.1 \times 10^{32}$	39.8	$<2.9 \times 10^{28}$	J04
GS 2000+25	2.7 ± 0.7	K3/K7V	1.6×10^{30}	30.7	$<2.2 \times 10^{27}$	G01
XTE J2012+381				47.4		

Notes. Distances taken from Jonker & Nelemans (2004) except for XTE J1908+094, which is taken from Jonker et al. (2004). Stellar spectral types are taken from McClintock & Remillard (2006). Quiescent X-ray luminosities are taken from the following references.
References. G01: Garcia et al. 2001; M03: McClintock et al. 2003; K02: Kong et al. 2002; H03: Hameury et al. 2003; P08: Pszota et al. 2008; C10: Calvelo et al. 2010; M99: Menou et al. 1999; T03: Tomsick et al. 2003; J04: Jonker et al. 2004.

2005b). The fitted correlation in Figure 1 shows that the three sources observed with the EVLA could just have been detected if they were as bright as A0620-00 at a similar X-ray luminosity. However, when taking into account the known variability in quiescent luminosity and the uncertainties in source distances and the fitted correlation index, we cannot definitively state that the sources are more radio faint in quiescence than expected.

4.1. Uncertainties

4.1.1. Source Variability

Quiescent X-ray binaries are known to be variable across the electromagnetic spectrum, from the X-ray (Corbel et al. 2006) through the optical (Cantrell et al. 2010) and radio bands (Miller-Jones et al. 2008). While the lowest-luminosity quiescent system with existing radio and X-ray detections (A0620-00; Gallo et al. 2006) was observed simultaneously in both bands, the new radio observations reported in this Letter were not simultaneous with the X-ray observations used in plotting our seven systems on the radio/X-ray luminosity correlation shown in Figure 1. For GRO J0422+322 and GRO J1655−40, some of the X-ray observations were taken 10 years prior to our EVLA data (Garcia et al. 2001). GRO J1655−40 has been particularly well studied in the X-ray band during its quiescent state (Garcia et al. 2001; Kong et al. 2002; Hameury et al. 2003; Pszota et al. 2008; Calvelo et al. 2010), showing a 3–9 keV X-ray flux that varied by a factor of more than five over the course of 9 years (Figure 1).

4.1.2. Distance Uncertainties

The distances to X-ray binaries are typically uncertain by 50% or more (Jonker & Nelemans 2004), adding an additional source of uncertainty to the derived X-ray and radio luminosities. Since the radio/X-ray correlation of (Gallo et al. 2003) is nonlinear ($L_{\rm R} \propto L_{\rm X}^{0.7}$), an error in the assumed distance could cause a source to appear artificially bright or faint in the radio band for its X-ray luminosity. Figure 1 shows the effect of the distance uncertainties on the sources forming the radio/X-ray correlation. Distance estimates and uncertainties come from Jonker & Nelemans (2004), except for GX 339−4 (6–15 kpc; Hynes et al. 2004), V404 Cyg (2.39 ± 0.14 kpc; Miller-Jones et al. 2009), H1743-322, and XTE J1908+094 (assumed Galactic Center distance of 8.5 kpc with an uncertainty of 2 kpc for both).

4.1.3. Correlation Index

Different authors, by considering different samples, have found different power-law indices for the radio/X-ray correlation. The original "universal" correlation found by Gallo et al. (2003) had a correlation index of 0.70 ± 0.20, whereas the addition of the A0620-00 point refined the index to 0.58 ± 0.16 (Gallo et al. 2006). Corbel et al. (2008) found an index of 0.51 ± 0.06 for V404 Cyg taken alone, although such a shallow correlation is ruled out by both the A0620-00 detection and our new data. However, the lack of low-luminosity radio detections prevents the correlation index being better constrained, with this uncertainty leading to significant variation in the predicted radio brightnesses of quiescent sources. Furthermore, it is not clear whether the measured relationship between X-ray and radio luminosity should indeed be a single, unbroken power law down to the lowest quiescent luminosities, as has been inferred from the simultaneous radio and X-ray detection of A0620-00 (Gallo et al. 2006). Advection-dominated accretion flow models predict a gradual softening of the power-law photon index in the X-ray band as a source decays to quiescence (e.g., Esin et al. 1997). That softening necessarily leads to changes in the fraction of the accretion luminosity arising in a given X-ray band. Even if the underlying relationship between accretion luminosity and jet emission were indeed a single power law, these changes would cause a slight deviation from the underlying power law in any empirical measurement of that relationship. Equally, as discussed in Section 1, synchrotron-dominated jet models predict a steepening of the relation below a critical X-ray luminosity (Yuan & Cui 2005), although such models do not seem to be applicable to either A0620-00 or Sgr A*.

In summary, the combination of uncertainties in quiescent X-ray luminosity, source distance, and correlation index is sufficient to explain the non-detections of all three of the sources we observed with the EVLA. As Figure 1 shows, when considering these uncertainties, none of the three sources observed with the EVLA fall significantly below the radio/X-ray correlation fitted by Gallo et al. (2006), which used the A0620-00 detection to constrain the correlation index down to the lowest luminosities. Thus our upper limits cannot be used to robustly constrain models for the radio/X-ray coupling in quiescence.

4.2. Stellar Radio Emission

At the sensitivity levels achieved in our EVLA observations, we are reaching the regime where stellar radio emission might be expected to contribute to the radio brightness of the sources. Güdel (2002) showed that the peak luminosities of incoherent gyrosynchrotron emission from stellar radio flares can reach 10^{18} erg s^{-1} Hz^{-1} for RS CVn, FK Com, and Algol systems. At the distance of the closest of our systems, XTE J1118+480 (Table 2), this corresponds to a radio flux density of 0.25 mJy beam^{-1}. However, our lack of detections suggests that any stellar emission is significantly fainter than this.

The spectral types of the donor stars for our target sources are listed in Table 2. The mass donors for the three sources observed with the EVLA are all late-type main sequence or subgiant stars. Typical radio luminosities for early/mid K stars are in the range 1×10^{14}–3×10^{15} erg s^{-1} Hz^{-1}, with the higher end of the range corresponding to the most rapid rotators. Although our X-ray binary targets will be tidally locked (with orbital periods in the range 4.1–62.9 hr), there is little correlation between rotation rate and radio flux density in dwarf stars (Güdel 2002), so the high rotation speeds should have minimal effect. We would therefore expect radio flux densities of $<2.5\ \mu$Jy $(d/1\ \rm kpc)$ from the donor stars. While for astrometric purposes the source of the radio emission is unimportant, stellar emission could begin to confuse the radio/X-ray luminosity correlation should we push deeper on these quiescent systems.

5. CONCLUSIONS

We have made deep VLA observations of the fields surrounding 11 confirmed or candidate black hole X-ray binaries. The only source detected was Swift J1753.5−0127, at a level of 0.4–0.5 mJy beam^{-1}. The typical 3σ upper limits on the radio brightnesses of the remaining sources were in the range 30–50 μJy beam^{-1}. Three targets were selected for follow-up with the EVLA, using 2 GHz of bandwidth to enhance the sensitivity. We found 3σ upper limits of 7.8, 8.3, and 14.2 μJy beam^{-1} for XTE J1118+480, GRO J0422+322, and GRO J1655−40, respectively. We find that most quiescent systems are beyond the reach of current high-sensitivity VLBI arrays, and cannot therefore be used as astrometric targets. Uncertainties in the source distances (Jonker & Nelemans 2004), in the empirical correlation between radio and X-ray emission, and in the X-ray luminosities at the times of the observations imply that we cannot rule out these sources falling on the radio/X-ray correlation of Gallo et al. (2003). However, while deeper constraints on the quiescent jet emission will be possible on completion of the EVLA, the existing upper limits suggest that it may be difficult to disentangle jet emission from stellar radio emission at such low radio luminosities.

J.C.A.M.-J. thanks Stephane Corbel for making available his original data on GX339−4. The National Radio Astronomy Observatory is a facility of the National Science Foundation operated under cooperative agreement by Associated Universities, Inc. This research has made use of NASA's Astrophysics Data System.

Facilities: EVLA, VLA

REFERENCES

Blandford, R. D., & Begelman, M. C. 1999, MNRAS, 303, L1
Blandford, R. D., & Konigl, A. 1979, ApJ, 232, 34
Calvelo, D. E., Fender, R. P., Russell, D. M., et al. 2010, MNRAS, 409, 839
Cantrell, A. G., Bailyn, C. D., Orosz, J. A., et al. 2010, ApJ, 710, 1127
Corbel, S., Körding, E., & Kaaret, P. 2008, MNRAS, 389, 1697
Corbel, S., Nowak, M. A., Fender, R. P., Tzioumis, A. K., & Markoff, S. 2003, A&A, 400, 1007
Corbel, S., Tomsick, J. A., & Kaaret, P. 2006, ApJ, 636, 971

Coriat, M., Corbel, S., Prat, L., et al. 2011, MNRAS, 414, 677
Esin, A. A., McClintock, J. E., & Narayan, R. 1997, ApJ, 489, 865
Falcke, H., Körding, E., & Markoff, S. 2004, A&A, 414, 895
Fender, R. P., Gallo, E., & Jonker, P. G. 2003, MNRAS, 343, L99
Gallo, E. 2007, in AIP Conf. Proc. 924, The Multicolored Landscape of Compact Objects and Their Explosive Origin, ed. L. A. Antonelli et al. (Melville, NY: AIP), 715
Gallo, E., Fender, R., Kaiser, C., et al. 2005a, Nature, 436, 819
Gallo, E., Fender, R. P., & Hynes, R. I. 2005b, MNRAS, 356, 1017
Gallo, E., Fender, R. P., Miller-Jones, J. C. A., et al. 2006, MNRAS, 370, 1351
Gallo, E., Fender, R. P., & Pooley, G. G. 2003, MNRAS, 344, 60
Garcia, M. R., McClintock, J. E., Narayan, R., et al. 2001, ApJ, 553, L47
Greisen, E. W. 2003, in Information Handling in Astronomy: Historical Vistas, ed. A. Heck (Dordrecht: Kluwer), 109
Güdel, M. 2002, ARA&A, 40, 217
Gültekin, K., Cackett, E. M., Miller, J. M., et al. 2009, ApJ, 706, 404
Hameury, J.-M., Barret, D., Lasota, J.-P., et al. 2003, A&A, 399, 631
Hynes, R. I., Steeghs, D., Casares, J., Charles, P. A., & O'Brien, K. 2004, ApJ, 609, 317
Jonker, P. G., Gallo, E., Dhawan, V., et al. 2004, MNRAS, 351, 1359
Jonker, P. G., & Nelemans, G. 2004, MNRAS, 354, 355
Jonker, P. G., Miller-Jones, J., Homan, J., et al. 2010, MNRAS, 401, 1255
Kong, A. K. H., McClintock, J. E., Garcia, M. R., Murray, S. S., & Barret, D. 2002, ApJ, 570, 277
McClintock, J. E., Narayan, R., Garcia, M. R., et al. 2003, ApJ, 593, 435
McClintock, J. E., & Remillard, R. A. 2006, in Compact Stellar X-ray Sources, ed. W. H. G. Lewin & M. van der Klis (Cambridge: Cambridge Univ. Press), 157
McMullin, J. P., Waters, B., Schiebel, D., Young, W., & Golap, K. 2007, in ASP Conf. Ser. 376, Astronomical Data Analysis Software and Systems XVI, ed. R. A. Shaw, F. Hill, & D. J. Bell (San Francisco, CA: ASP), 127
Menou, K., Esin, A. A., Narayan, R., et al. 1999, ApJ, 520, 276
Merloni, A., Heinz, S., & di Matteo, T. 2003, MNRAS, 345, 1057
Miller-Jones, J. C. A., Gallo, E., Rupen, M. P., et al. 2008, MNRAS, 388, 1751
Miller-Jones, J. C. A., Jonker, P. G., Dhawan, V., et al. 2009, ApJ, 706, L230
Mirabel, I. F., Dhawan, V., Mignani, R. P., Rodrigues, I., & Guglielmetti, F. 2001, Nature, 413, 139
Mirabel, I. F., & Rodrigues, I. 2003, Science, 300, 1119
Narayan, R., Igumenshchev, I. V., & Abramowicz, M. A. 2000, ApJ, 539, 798
Narayan, R., & Yi, I. 1995, ApJ, 452, 710
Perley, R. A., Chandler, C. J., Butler, B. J., & Wrobel, J. M. 2011, ApJ, 739, L1
Pszota, G., Zhang, H., Yuan, F., & Cui, W. 2008, MNRAS, 389, 423
Quataert, E., & Gruzinov, A. 2000, ApJ, 539, 809
Sault, R. J., & Wieringa, M. H. 1994, A&AS, 108, 585
Soleri, P., Fender, R., Tudose, V., et al. 2010, MNRAS, 406, 1471
Tomsick, J. A., Corbel, S., Fender, R., et al. 2003, ApJ, 597, L133
Yuan, F., & Cui, W. 2005, ApJ, 629, 408